NEURODEVELOPMENT

Reciprocal repulsions instruct the precise assembly of parallel hippocampal networks

Daniel T. Pederick[1], Jan H. Lui[1], Ellen C. Gingrich[1,2], Chuanyun Xu[1], Mark J. Wagner[1], Yuanyuan Liu[3]†, Zhigang He[3], Stephen R. Quake[4,5], Liqun Luo[1]*

Mammalian medial and lateral hippocampal networks preferentially process spatial- and object-related information, respectively. However, the mechanisms underlying the assembly of such parallel networks during development remain largely unknown. Our study shows that, in mice, complementary expression of cell surface molecules teneurin-3 (Ten3) and latrophilin-2 (Lphn2) in the medial and lateral hippocampal networks, respectively, guides the precise assembly of CA1-to-subiculum connections in both networks. In the medial network, Ten3-expressing (Ten3+) CA1 axons are repelled by target-derived Lphn2, revealing that Lphn2- and Ten3-mediated heterophilic repulsion and Ten3-mediated homophilic attraction cooperate to control precise target selection of CA1 axons. In the lateral network, Lphn2-expressing (Lphn2+) CA1 axons are confined to Lphn2+ targets via repulsion from Ten3+ targets. Our findings demonstrate that assembly of parallel hippocampal networks follows a "Ten3→Ten3, Lphn2→Lphn2" rule instructed by reciprocal repulsions.

Parallel information processing is a salient feature of complex nervous systems. One example is the mammalian hippocampal-entorhinal network, which is essential for explicit memory formation and spatial representation (*1*–*4*). Spatial- and object-related information are preferentially processed by the medial and lateral hippocampal networks, respectively (*5*, *6*). In the medial network, proximal CA1 axons project to the distal subiculum (Fig. 1A, cyan), and both proximal CA1 and the distal subiculum also form reciprocal connections with the medial entorhinal cortex. In the lateral network, distal CA1 axons project to the proximal subiculum (Fig. 1A, yellow), and both distal CA1 and the proximal subiculum form reciprocal connections with the lateral entorhinal cortex (*7*, *8*) (fig. S1A).

We previously showed that the type II transmembrane protein teneurin-3 (Ten3) has matching expression in all interconnected regions of the medial hippocampal network (*9*). Ten3 is required in both proximal CA1 and the distal subiculum for target selection of the proximal CA1→distal subiculum axons, and it promotes aggregation of nonadhesive cells (*9*). These data support a homophilic attraction mechanism by which Ten3 regulates target selection in the medial hippocampal network. It remains unclear whether matching gene expression exists in the lateral hippocampal network and how this contributes to parallel hippocampal network assembly.

[1]Department of Biology, Howard Hughes Medical Institute, Stanford University, Stanford, CA, USA. [2]Neurosciences Graduate Program, Stanford University, Stanford, CA, USA. [3]F.M. Kirby Neurobiology Center, Department of Neurology, Boston Children's Hospital, Harvard Medical School, Boston, MA, USA. [4]Departments of Bioengineering and Applied Physics, Stanford University, Stanford, CA, USA. [5]Chan Zuckerberg Biohub, Stanford, CA, USA.
*Corresponding author. Email: lluo@stanford.edu
†Present address: Somatosensation and Pain Unit, National Institute of Dental and Craniofacial Research (NIDCR), National Center for Complementary and Integrative Health (NCCIH), National Institutes of Health, Bethesda, MD, USA.

Complementary Lphn2/Ten3 expression across parallel hippocampal networks

We hypothesized that cell surface molecules with expression patterns inverse to those of *Ten3*, and therefore enriched in the lateral hippocampal network, may play a role in the precise assembly of parallel hippocampal networks. To identify such genes, we performed fluorescence-activated cell sorting–based single-cell RNA sequencing of postnatal day 8 (P8) excitatory neurons that express vesicular glutamate transporter 1 in subregions of the medial or lateral networks (figs. S1 and S2). Among cell surface molecules that are differentially expressed in CA1 and the subiculum (fig. S3A), we identified *latrophilin-2* (*Lphn2*), an adhesion G protein–coupled receptor known to bind teneurins (*10*–*15*), which showed expression inverse to that of *Ten3*, not only in CA1 and the subiculum but also in the entorhinal cortex (Fig. 1B, fig. S4A, and table S1). Other *teneurin* and *latrophilin* family members did not display such differential expression (fig. S3, B and C).

Double in situ hybridization for *Lphn2* and *Ten3* mRNA in the P8 mouse brain revealed preferential expression of *Lphn2* in distal CA1, the proximal subiculum, and the lateral entorhinal cortex, complementary to *Ten3* enrichment in proximal CA1, the distal subiculum, and the medial entorhinal cortex (Fig. 1, C and D, and fig. S4, B and C). We also examined protein expression by using an anti-Ten3 antibody (*9*) and an anti–green fluorescent protein (GFP) antibody in *Lphn2-mVenus* knock-in mice (*16*). In all regions, Lphn2 and Ten3 proteins were expressed in the synaptic layers corresponding to their mRNA expression, including the molecular layer of CA1, the cell body and molecular layers of the subiculum, and layer III of the entorhinal cortex (Fig. 1, E and F, and fig. S4, D and E). Thus, *Lphn2* and *Ten3* mRNA, as well as Lphn2 and Ten3 proteins, exhibit complementary expression in multiple regions of the developing hippocampal networks, including CA1, the subiculum, and the entorhinal cortex (fig. S4F). In all cases, the connection specificity follows a "Ten3→Ten3, Lphn2→Lphn2" rule that correlates cell surface molecule expression with connectivity.

In the rest of this study, we focused on the target selection of CA1→subiculum axons to investigate the developmental mechanisms by which the "Ten3→Ten3, Lphn2→Lphn2" rule is established. Ten3+ and Lphn2+ CA1 axons extend along a tract above the subiculum cell body layer until they reach the Ten3+ distal subiculum and Lphn2+ proximal subiculum, respectively, where they invade the cell body layer of the subiculum to form synapses (*9*) (fig. S5). Lphn2 and Ten3 proteins were first detected in subiculum targets (by P2) and displayed increasing expression in CA1 in subsequent days. By P8, the highest levels of Lphn2 and Ten3 in CA1 and the subiculum are comparable (fig. S6). This increase in expression coincides with the timing of target selection of CA1 axons in the subiculum (*9*).

Subiculum Lphn2 repels Ten3+ CA1 axons

Ten3 directs axon targeting in the medial hippocampal network through matching expression and homophilic attraction (*9*). Does Lphn2 also mediate homophilic attraction to assemble the lateral hippocampal network? To test this, we performed an in vitro cell aggregation assay using nonadhesive K562 cells. We confirmed that Ten3-expressing K562 cells formed aggregates, as previously reported (*9*), but found that Lphn2-expressing cells did not (fig. S7, A and B). However, Ten3-expressing cells aggregated with Lphn2-expressing cells (fig. S7, A and B), consistent with the previously reported heterophilic interaction between teneurins and latrophilins (*10*–*15*). The heterophilic interaction of Ten3 and Lphn2, combined with their complementary expression in the medial versus lateral hippocampal network, suggests that the interaction between Lphn2 and Ten3 may result in repulsion, which could allow distinct target selection of axons in the medial and lateral hippocampal networks.

The CA1→subiculum projection develops postnatally (*9*), so we injected lentivirus expressing *GFP* (control) or *GFP-P2A-Lphn2* into the Lphn2-low distal subiculum of mice at P0 to create a region of the subiculum expressing Lphn2 across the entire proximal-distal axis. We then injected adeno-associated virus expressing membrane-bound mCherry (*AAV-mCh*) into proximal CA1 in these same mice as adults to label and trace Ten3+ CA1 axons (Fig. 2, A and B). The portion of the subiculum transduced by lentivirus was only a subset of the total proximal CA1 axon targeting

region along the orthogonal medial-lateral axis, allowing us to determine whether proximal CA1 axons target lentivirus-transduced subiculum regions differently compared with neighboring non–lentivirus-transduced subiculum regions.

To visualize the relationship between Ten3+ axon projections and ectopically expressed GFP-Lphn2 in the subiculum, we plotted signal intensity from proximal CA1 axons (mCh) and the lentivirus injection site (GFP) on the same subiculum graph as color and height, respectively. Expression of GFP alone did not affect the intensity of proximal CA1 axons in the subiculum target (Fig. 2C and fig. S8, A to C). However, proximal CA1 axon intensity was reduced in distal subiculum regions ectopically expressing Lphn2 (Fig. 2D and fig. S8, D to F; quantified in Fig. 2G). These data suggest that Ten3+ axons are repelled by ectopically expressed Lphn2 at the distal subiculum target.

Repulsion requires Lphn2/teneurin but not Lphn2/FLRT interaction

To test whether Lphn2-mediated repulsion requires Lphn2 and Ten3 (Lphn2/Ten3) interaction, we used a deletion of the lectin binding domain in latrophilins, which has been shown to abolish teneurin binding without affecting cell surface expression or interactions with other known partners (*12*–*15*). In our K562 cell aggregation assay, we validated that Lphn2_ΔLec disrupted Ten3 interaction without affecting interaction with FLRT2 (fig. S7, C and D), a member of the fibronectin leucine-rich transmembrane protein family known to bind latrophilins (*11*, *17*). We then ectopically expressed Lphn2_ΔLec in the subiculum to determine whether proximal CA1 axon avoidance depends on a Lphn2/teneurin interaction. We found that in brains ectopically expressing *GFP-P2A-Lphn2_ΔLec*, Ten3+ proximal CA1 axons no longer avoided Lphn2_ΔLec-expressing regions in the distal subiculum (Fig. 2E and fig. S9, A to C; quantified in Fig. 2G).

FLRTs interact with teneurin and latrophilin to direct synapse specificity and repulsive guidance for migrating neurons (*14*, *15*). Expression of *Flrt2* was enriched in Ten3-high CA1 cells (fig. S3D), suggesting that it may play a role in the repulsion of proximal CA1 axons by target-derived Lphn2. Mutation of four residues in the olfactomedin domain of latrophilin to alanines abolishes FLRT-Lphn binding while maintaining cell surface expression and teneurin binding (*18*). We confirmed that in K562 cells, Lphn2_4A disrupted FLRT2 binding without affecting Ten3 binding (fig. S7, E and F). Yet ectopic expression of Lphn2_4A in the subiculum caused a decrease of Ten3+ proximal CA1 axon intensity in GFP+ distal subiculum regions compared with adjacent GFP– regions (Fig. 2F and fig. S9, D to F; quantified in Fig. 2G), to the same extent as wild-type Lphn2 (Fig. 2G). These gain-of-function experiments suggest that repulsion of Ten3+ proximal CA1 axons by target-derived Lphn2 requires Lphn2/teneurin but not Lphn2/FLRT interaction.

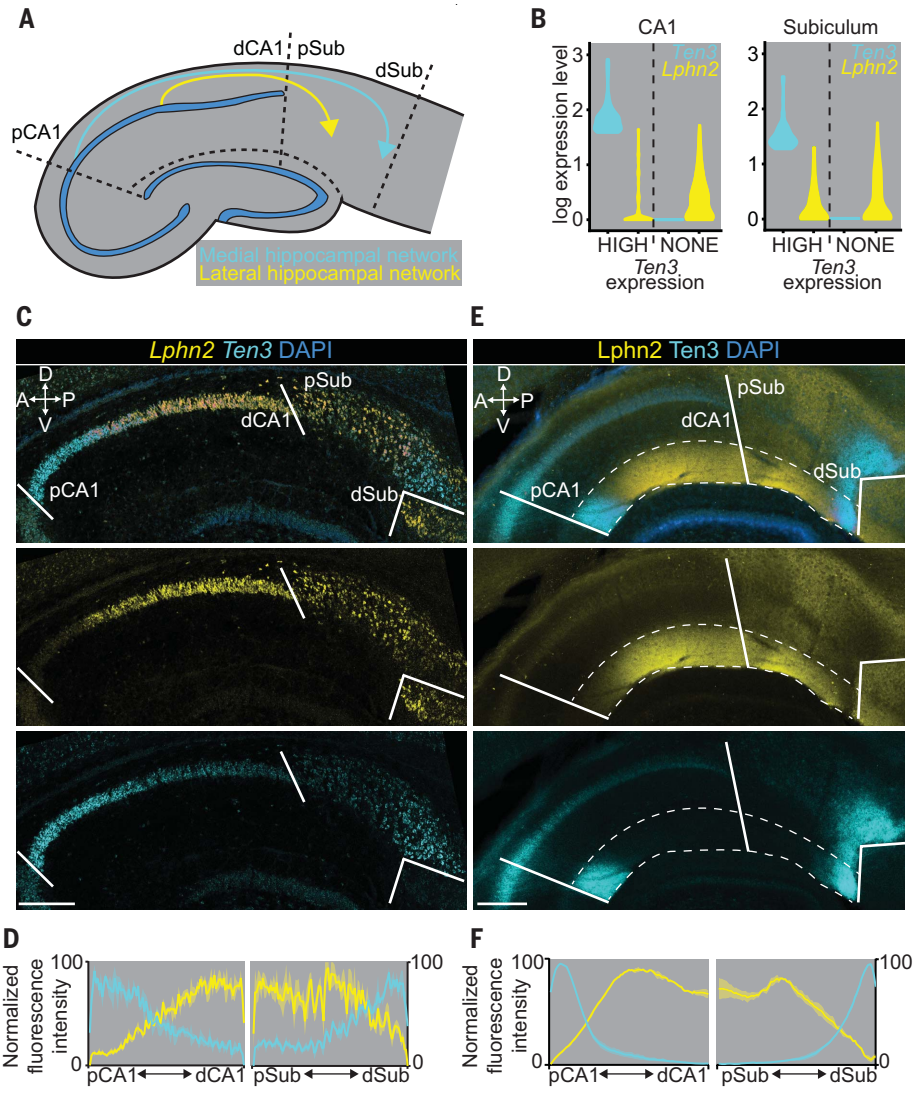

Fig. 1. Complementary expression patterns of Lphn2 and Ten3 in the hippocampal network. (**A**) Summary of connection patterns of medial (cyan) and lateral (yellow) hippocampal networks. pCA1 and dCA1, proximal and distal CA1; pSub and dSub, proximal and distal subiculum. (**B**) Violin plots highlighting *Lphn2* and *Ten3* expression in *Ten3*-HIGH and *Ten3*-NONE cells in CA1 and the subiculum. The unit of expression level is ln[1+ (reads per 10,000 transcripts)]. (**C**) Double in situ hybridization for *Lphn2* (middle) and *Ten3* (bottom) mRNA on a sagittal section of P8 mouse brain. Solid lines represent boundaries between CA1 and the subiculum, as labeled in the overlay (top). DAPI, 4′,6-diamidino-2-phenylindole. (**D**) Quantification of *Lphn2* and *Ten3* mRNA across the proximal-distal axis of CA1 and subiculum cell body layers (n = 3 mice). Means ± SEMs are shown. (**E**) Double immunostaining for Lphn2 (middle; anti-GFP antibody) and Ten3 (bottom) on a sagittal section of P8 *Lphn2-mVenus* knock-in mouse (*16*) brain. Solid lines represent boundaries between CA1 and the subiculum, as labeled in the overlay (top). The region between the dashed lines is the molecular layer. (**F**) Quantification of Lphn2 and Ten3 protein across the proximal-distal axis of molecular layers of CA1 and the subiculum (n = 3 mice). Means ± SEMs are shown. Scale bars in (C) and (E), 200 μm. Axis labels in this and all subsequent figures: A, anterior; P, posterior; D, dorsal; V, ventral.

Ten3+ CA1 axons invade *Lphn2*-null subiculum targets

To determine whether endogenous *Lphn2* in the subiculum is necessary for correct proximal CA1→distal subiculum targeting, we performed a loss-of-function experiment by injecting lentivirus expressing *GFP-Cre* into the subiculum of control and *Lphn2*$^{fl/fl}$ mice (*16*) at P0, followed by *AAV-mCh* in proximal CA1 of the same mice as adults to assess Ten3+ axon targeting (Fig. 3, A and C). In *Lphn2*$^{+/+}$ control mice, proximal CA1 axons targeted the distal subiculum and were not disrupted when projecting into GFP-Cre+ regions (Fig. 3B). By contrast, proximal CA1 axons

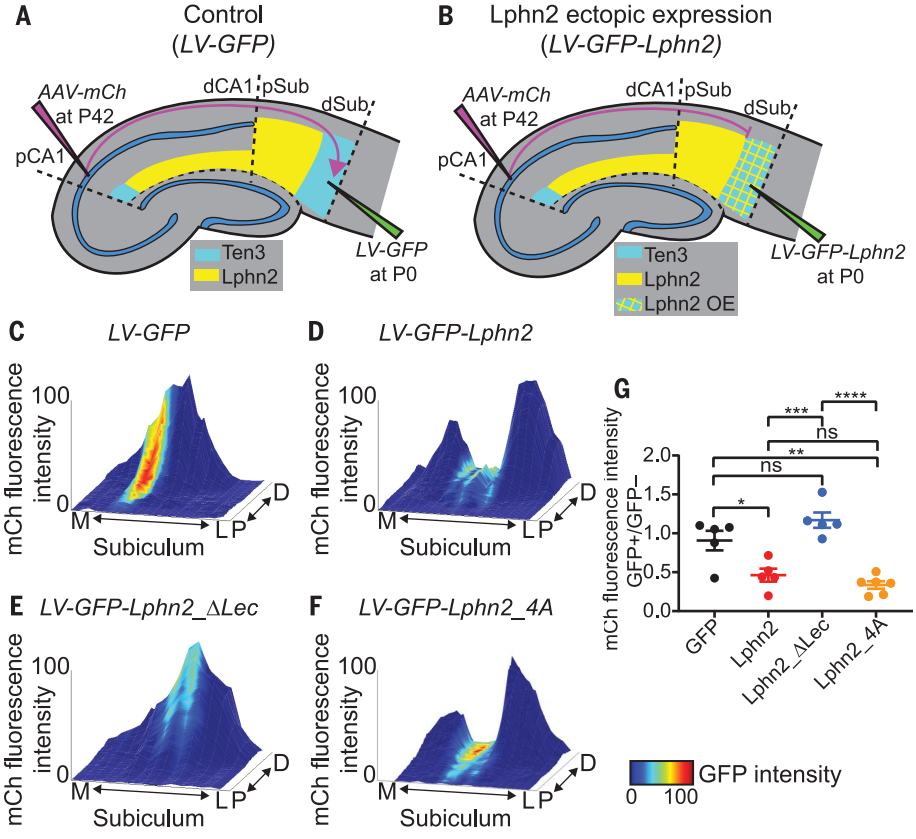

Fig. 2. Ten3+ proximal CA1 axons avoid the distal subiculum ectopically expressing Lphn2 in a Lphn2/teneurin interaction–dependent and Lphn2/FLRT interaction–independent manner. (**A** and **B**) Experimental design and summary of results. LV, lentivirus; *AAV-mCh*, adeno-associated virus expressing membrane-bound mCherry as an anterograde tracer. (**C** to **F**) Representative mountain plots showing normalized GFP fluorescence intensity as color (LV expression) and normalized mCh fluorescence intensity as height (proximal CA1 axon projections) in the subiculum. P, proximal; D, distal; M, medial; L, lateral. (**G**) Ratio of mCh fluorescence intensity of GFP+ versus GFP− regions. *LV-GFP*, n = 5 mice; *LV-GFP-P2A-Lphn2* (wild-type Lphn2), n = 5 mice; *LV-GFP-P2A-Lphn2_ΔLec* (Lphn2 that does not bind teneurins), n = 5 mice; and *LV-GFP-P2A-Lphn2_4A* (Lphn2 that does not bind FLRTs), n = 6 mice. Means ± SEMs are shown; one-way analysis of variance (ANOVA) with Tukey's multiple comparisons test was performed. ****$P \le 0.0001$; ***$P \le 0.001$; **$P \le 0.01$; *$P \le 0.05$; ns, not significant.

targeted more broadly in GFP-Cre+ regions in *Lphn2*$^{fl/fl}$ mice (Fig. 3D). Quantification of proximal CA1 axon intensity in GFP-Cre+ sections revealed that proximal CA1 axons in *Lphn2*$^{fl/fl}$ mice had increased intensity in the more proximal regions and decreased intensity in the most distal region of the subiculum compared with *Lphn2*$^{+/+}$ mice (Fig. 3, G and H; red versus black). These data suggest that Lphn2 in the proximal subiculum normally repels Ten3+ proximal CA1 axons, enabling them to specifically target the distal subiculum.

To rule out the possibility that the ectopic invasion of proximal CA1 axons into the *Lphn2*$^{-/-}$ proximal subiculum results from loss of Lphn2 interaction with a molecule other than Ten3 [e.g., another teneurin that is expressed in CA1 (fig. S3B)], we performed the same *Lphn2* loss-of-function experiment in *Ten3*$^{-/-}$ mice. Anterograde tracing from proximal CA1 in *Lphn2*$^{+/+}$;*Ten3*$^{-/-}$ mice showed that proximal CA1 axons spread more along the proximal-distal axis of the subiculum (fig. S10, A and B). In *Lphn2*$^{fl/fl}$;*Ten3*$^{-/-}$ mice, proximal CA1 axons also showed similar spreading (fig. S10, C and D; quantified in fig. S10, E and F). The lack of an additional axon mistargeting phenotype in *Lphn2*$^{fl/fl}$;*Ten3*$^{-/-}$ mice compared with *Lphn2*$^{+/+}$;*Ten3*$^{-/-}$ mice suggests that Ten3 is required for the effect of loss of subiculum Lphn2 on proximal CA1 axon targeting and that Lphn2/Ten3-mediated repulsion instructs proximal CA1→distal subiculum target selection.

Lphn2/Ten3-mediated repulsion and Ten3/Ten3-mediated attraction cooperate

Loss of Lphn2/Ten3 heterophilic repulsion (above) or Ten3 homophilic attraction (*9*) alone both disrupt precise proximal CA1→distal subiculum axon targeting. What is the relative contribution of each? To address this, we simultaneously conditionally deleted both *Lphn2* and *Ten3* in the subiculum and assessed the targeting of Ten3+ proximal CA1 axons (Fig. 3E). We found that proximal CA1 axons projecting into GFP-Cre+ regions of *Lphn2*$^{fl/fl}$;*Ten3*$^{fl/fl}$ mice targeted more proximal regions of the subiculum and also had decreased fluorescence intensity in the distal subiculum (Fig. 3F).

Quantification of proximal CA1 axons in GFP-Cre+ subiculum sections of *Lphn2*$^{fl/fl}$;*Ten3*$^{fl/fl}$ mice showed a significant increase in axon intensity into the *Lphn2*$^{-/-}$ proximal subiculum compared with axons in *Lphn2*$^{+/+}$;*Ten3*$^{+/+}$ mice (Fig. 3, G and H; blue versus black), confirming a loss of repulsion of Ten3+ proximal CA1 axons from the proximal subiculum that normally expresses Lphn2. Additionally, proximal CA1 axons in *Lphn2*$^{fl/fl}$;*Ten3*$^{fl/fl}$ mice had decreased fluorescence intensity in the distal subiculum compared with axons in *Lphn2*$^{fl/fl}$;*Ten3*$^{+/+}$ mice (Fig. 3, G and H; blue versus red), indicating a loss of attraction of Ten3+ proximal CA1 axons to the distal subiculum that normally expresses Ten3. Thus, Lphn2/Ten3-mediated heterophilic repulsion and Ten3/Ten3-mediated homophilic attraction cooperate in orchestrating the precise targeting of proximal CA1 axons to the distal subiculum.

Subiculum Ten3 repels Lphn2+ CA1 axons

In addition to serving as a repulsive ligand for target selection of Ten3+ medial hippocampal network neurons, could Lphn2 also act as a receptor to regulate target selection of lateral hippocampal network neurons? Could Lphn2+ axons be repelled from Ten3+ targets to regulate the precision of lateral hippocampal network connections? To test these ideas, we injected lentivirus expressing *GFP-Cre* into the subiculum of *Ten3*$^{+/+}$ (control) and *Ten3*$^{fl/fl}$ mice at P0, followed by *AAV-mCh* in mid-CA1 of the same mice as adults to assess Lphn2+ mid-CA1 axon targeting (Fig. 4, A and C). In *Ten3*$^{+/+}$ mice, mid-CA1 axons predominantly targeted the mid-subiculum (Fig. 4B). However, in *Ten3*$^{fl/fl}$ mice, mid-CA1 axons spread into the *Ten3*-null distal subiculum (Fig. 4D). Quantification of axons in the subiculum showed a significant increase in axon intensity in the distal subiculum of *Ten3*$^{fl/fl}$ mice compared with *Ten3*$^{+/+}$mice (Fig. 4, E and F). Thus, Ten3 in the distal subiculum prevents Lphn2+ mid-CA1 axon invasion into the distal subiculum.

To test whether Lphn2 in mid-CA1 axons is required for their target precision, we deleted *Lphn2* from CA1 and then traced *Lphn2*-null mid-CA1 axons (Fig. 4, G and I). Control mid-CA1 axons targeted the mid-subiculum (Fig. 4H), whereas *Lphn2*-null mid-CA1 axons spread into the most distal subiculum (Fig. 4J; quantified in Fig. 4, K and L). Thus, Lphn2 is cell-autonomously required in mid-CA1 neurons to

prevent their axons from invading the Ten3+ distal subiculum. Taken together with the *Ten3* conditional deletion in the subiculum above, these data indicate that Lphn2+ mid-CA1 axons are repelled by target-derived Ten3.

Discussion

In this study, we used CA1→subiculum axon targeting as a model to investigate how parallel networks are assembled during development. Our results demonstrate that Lphn2 and Ten3 instruct the precise assembly of both medial and lateral hippocampal networks (Fig. 5A). In the medial network, Lphn2/Ten3-mediated heterophilic repulsion and Ten3/Ten3-mediated homophilic attraction cooperate to instruct proximal CA1→distal subiculum axon targeting. In the lateral network, Ten3/Lphn2-mediated heterophilic repulsion confines Lphn2+ axons to the Lphn2+ target region (Fig. 5B). Additional cell surface molecules may further subdivide the Lphn2+ region to determine targeting specificity between mid-CA1→mid-subiculum and distal CA1→proximal subiculum. Together, these data indicate that the mechanisms required for parallel network assembly in the hippocampus are intertwined, using multiple interactions of two cell surface molecules and reciprocal repulsions to ensure the precise segregation of connections.

Our results reveal that Lphn2 acts both cell nonautonomously in targets and cell autonomously in axons during the target selection stage of hippocampal circuit assembly, preceding synapse formation. This is in contrast to previous studies suggesting that latrophilins act strictly as postsynaptic adhesion molecules to establish or maintain synaptic connections (*14*, *16*, *19*). Although defects in axon targeting may contribute to synaptic deficits in *latrophilin* early postnatal loss-of-function experiments (*14*, *16*, *20*), our study is compatible with latrophilin/teneurin interactions playing additional roles in synaptic adhesion if the repulsive mechanism is switched off after target selection is complete. While the most parsimonious interpretation is that the interactions between Lphn2 and Ten3 mediate repulsion directly, our study does not rule out the possibility that Lphn2/Ten3 interactions initiate signaling cascades that activate repulsive interactions mediated by additional molecules. Latrophilins bind both teneurins and FLRTs, and the cooperative binding of these three proteins has been implicated in directing synapse specificity and repulsion-mediated neuronal migration (*14*, *15*). However, ectopic expression of a mutant Lphn2 that cannot bind FLRT (fig. S7, E and F) still repelled Ten3+ proximal CA1 axons to the same extent (Fig. 2G), suggesting that FLRT binding is not required for Lphn2/Ten3-mediated repulsion during target selection of axons.

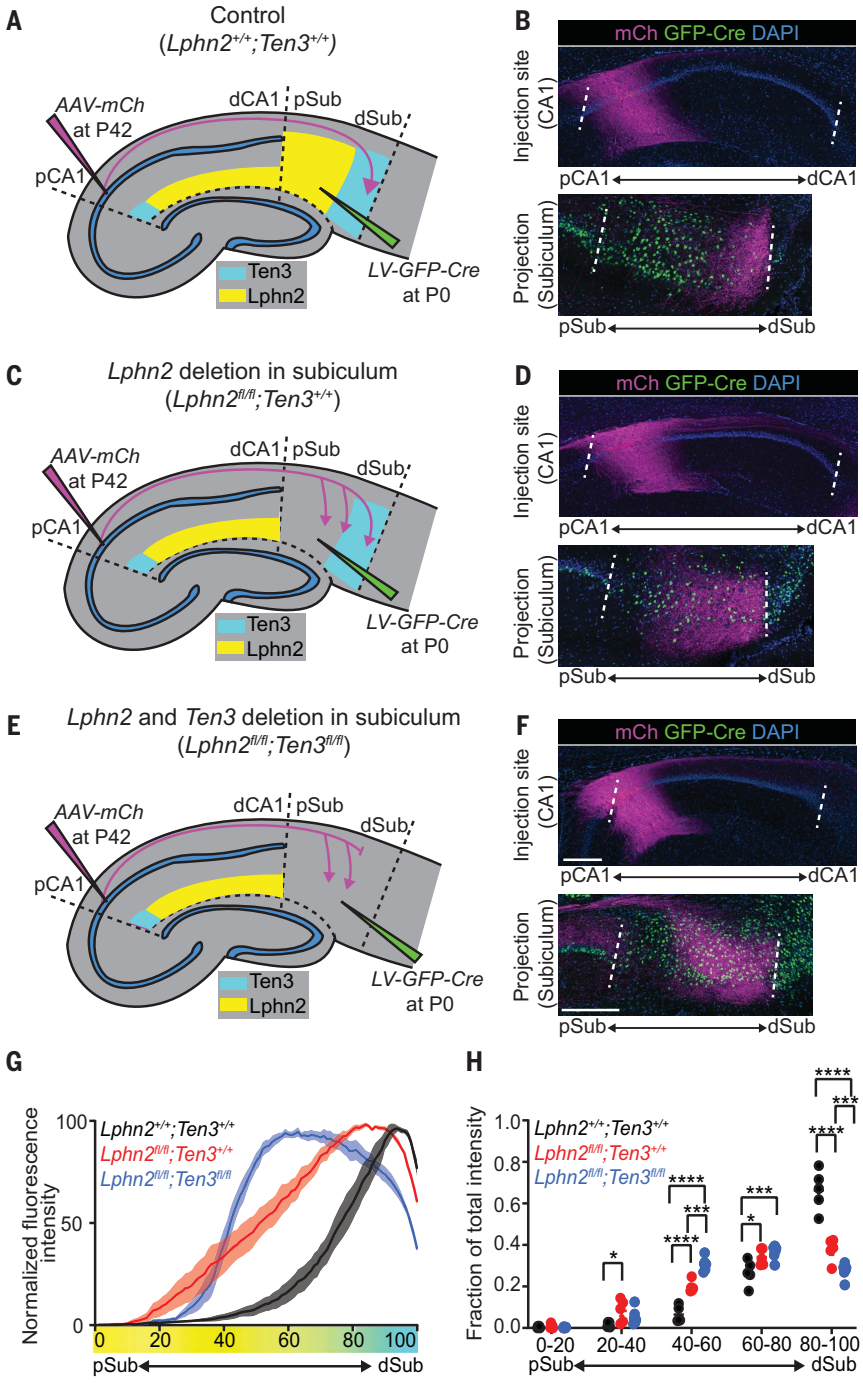

Fig. 3. Lphn2/Ten3-mediated repulsion and Ten3/Ten3-mediated attraction cooperate to guide proximal CA1→distal subiculum target selection. (**A, C,** and **E**) Experimental design and summary of results for control (A), *Lphn2* conditional knockout in the subiculum (C), and *Lphn2* and *Ten3* double conditional knockout in the subiculum (E). (**B**, **D,** and **F**) Representative images of *AAV-mCh* (magenta) injections in proximal CA1 (top) and corresponding projections of proximal CA1 axons overlapping with *LV-GFP-Cre* (green) injection sites in the subiculum (bottom). Data in (B), (D), and (F) correspond to experimental conditions in (A), (C), and (E), respectively. (**G**) Normalized mean fluorescence intensity traces of subiculum projections from proximal CA1 in GFP-Cre+ sections for $Lphn2^{+/+};Ten3^{+/+}$ mice (n = 5), $Lphn2^{fl/fl};Ten3^{+/+}$ mice (n = 5), and $Lphn2^{fl/fl};Ten3^{fl/fl}$ mice (n = 6). Means ± SEMs are shown. The color bar under the x axis represents Lphn2 (yellow) and Ten3 (cyan) expression in the subiculum, as quantified in Fig. 1F. (**H**) Fraction of total axon intensity for the same data as in (G) across 20% intervals. Means ± SEMs are shown; two-way ANOVA with Sidak's multiple comparisons test was performed. $^{****}P \le 0.0001$; $^{***}P \le 0.001$; $^{*}P \le 0.05$. Scale bars in (F), 200 μm. Injection site locations in CA1 are shown in fig. S11.

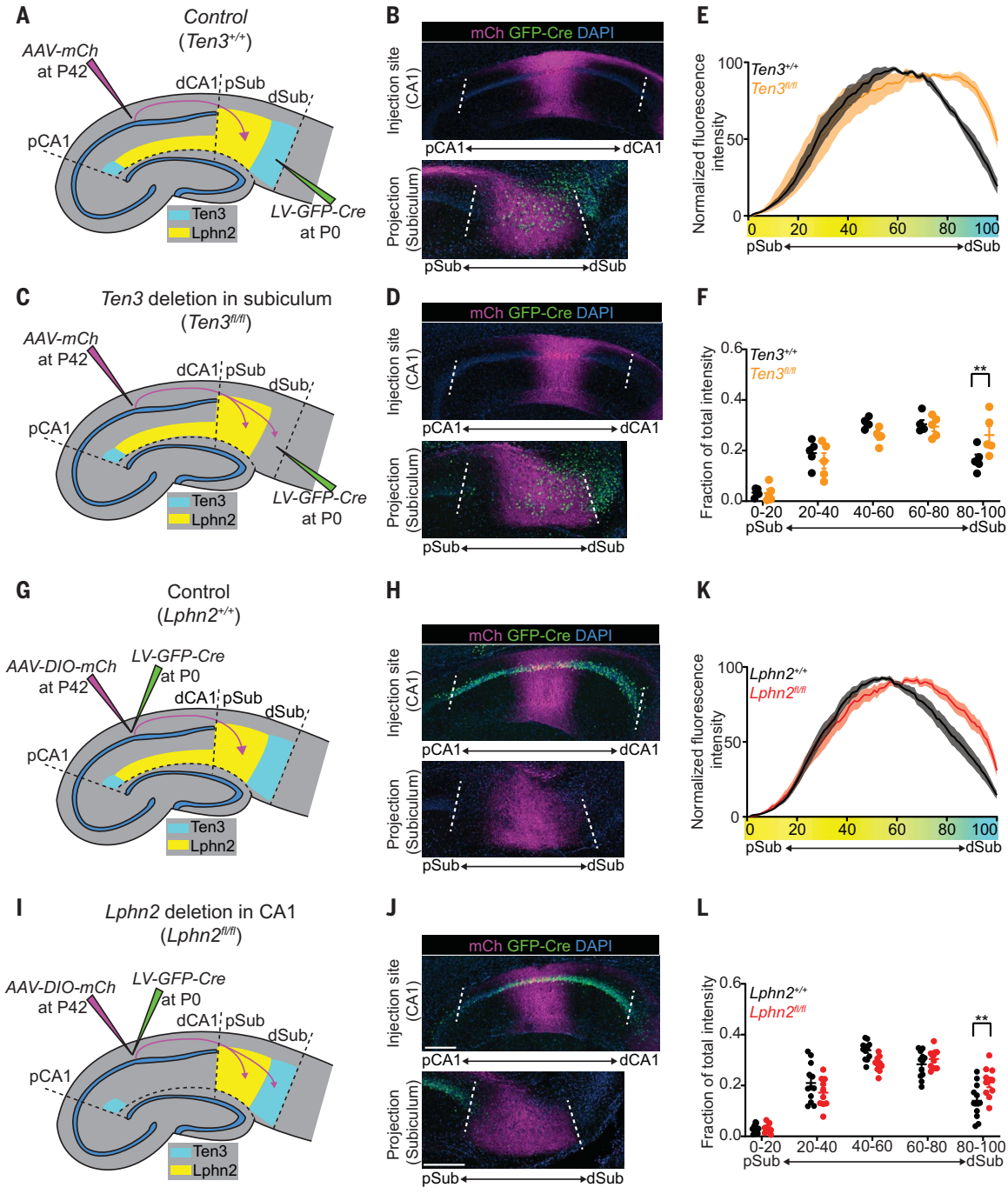

Fig. 4. Lphn2+ mid-CA1 axons avoid the Ten3+ distal subiculum. (**A** and **C**) Experimental design and summary of results for tracing mid-CA1 axons in control (A) and *Ten3* conditional knockout in the subiculum (C). (**B** and **D**) Representative images of *AAV-mCh* (magenta) injections in mid-CA1 (top) and corresponding projections overlapping with *LV-GFP-Cre* (green) injection sites in the subiculum (bottom). Data in (B) and (D) correspond to experimental conditions in (A) and (C), respectively. (**E**) Normalized mean fluorescence intensity traces of subiculum projections from mid-CA1 in GFP-Cre+ sections for $Ten3^{+/+}$ mice (n = 5) and $Ten3^{fl/fl}$ mice (n = 5). Means ± SEMs are shown. The color bar under the x axis represents Lphn2 (yellow) and Ten3 (cyan) expression in the subiculum, as quantified in Fig. 1F. (**F**) Fraction of total axon intensity [same data as in (E)] across 20% intervals. Means ± SEMs are shown; two-way ANOVA with Sidak's multiple comparisons test was performed. $^{**}P \leq 0.01$. (**G** and **I**) Experimental design and summary of results for tracing control (G) and *Lphn2*-null (I) mid-CA1 axon projections to the subiculum. (**H** and **J**) Representative images of *AAV-DIO-mCh* (magenta; mCh expression in a Cre-dependent manner) injections in mid-CA1 (top) and corresponding projections in the subiculum (bottom). Data in (H) and (J) correspond to experimental conditions in (G) and (I), respectively. (**K**) Normalized mean fluorescence intensity traces of subiculum projections from $Lphn2^{+/+}$ (n = 12 mice) and $Lphn2^{fl/fl}$ (n = 10 mice) mid-CA1 axons. Means ± SEMs are shown. The color bar under the x axis represents Lphn2 (yellow) and Ten3 (cyan) expression in the subiculum, as quantified in Fig. 1F. (**L**) Fraction of total axon intensity [same data as in (K)] across 20% intervals. Means ± SEMs are shown; two-way ANOVA with Sidak's multiple comparisons test was performed. $^{**}P \leq 0.01$. Scale bars in (J), 200 μm. Injection site locations in CA1 are shown in fig. S11.

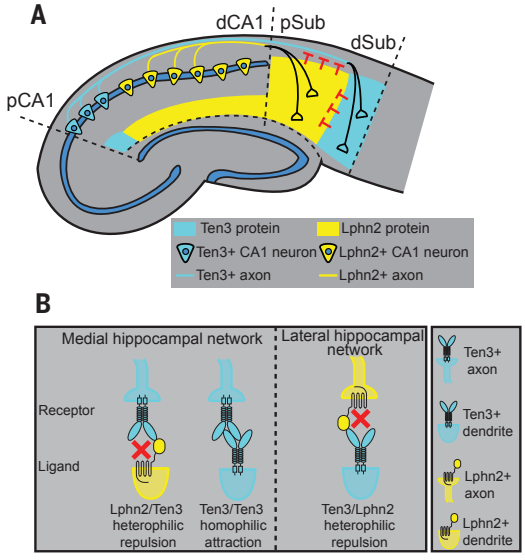

Fig. 5. Lphn2 and Ten3 instruct target selection of hippocampal axons through reciprocal repulsions. (**A**) Ten3+ CA1 axons target the Ten3+ subiculum via repulsion from Lphn2 and attraction to Ten3 in the subiculum. Lphn2+ CA1 axons target the Lphn2+ subiculum via repulsion from Ten3 in the subiculum. (**B**) Cartoon representation of ligand-receptor interactions that instruct target selection of Ten3+ (left) and Lphn2+ (right) axons. Red crosses symbolize repulsion.

Cooperation of attraction and repulsion has been described in neuronal circuit assembly (*21*, *22*). For example, the PlexB receptor interacts with Sema2a and Sema2b through repulsion and attraction, respectively, to mediate axon guidance during *Drosophila* sensory circuit assembly (*23*). We found that target selection of proximal CA1 axons is determined by Lphn2/Ten3-mediated repulsion from the proximal subiculum and Ten3/Ten3-mediated attraction to the distal subiculum (Fig. 3). Thus, Ten3 acts as a receptor for both repulsive and attractive ligands in the same axon during target selection. Conversely, as a ligand, Ten3 acts as an attractant for Ten3+ axons but a repellent for Lphn2+ axons (Fig. 5).

We show the complementary expression of Ten3 and Lphn2 across all interconnected regions of the hippocampal network. This is reminiscent of Ephrin-A/EphA countergradients found across interconnected regions of the developing visual system (*24*) that use bidirectional Ephrin-A/EphA interactions for the formation of topographic projections (*25*, *26*). The patterns of Ten3 and Lphn2 expression across the hippocampal network follow a "Ten3→Ten3, Lphn2→Lphn2" rule (fig. S4F). The reciprocal repulsions we demonstrated in the CA1→subiculum projection may guide target selection across additional projections to and from the entorhinal cortex. With repeated use in various connections combined with multifunctionality, in which a single protein serves as both receptor and ligand, a limited number of cell surface molecules can specify a diversity of connections in the mammalian brain.

REFERENCES AND NOTES

1. J. O'Keefe, J. Dostrovsky, *Brain Res.* **34**, 171–175 (1971).
2. W. B. Scoville, B. Milner, *J. Neuropsychiatry Clin. Neurosci.* **12**, 103–113 (2000).
3. L. R. Squire, C. E. L. Stark, R. E. Clark, *Annu. Rev. Neurosci.* **27**, 279–306 (2004).
4. T. Hafting, M. Fyhn, S. Molden, M.-B. Moser, E. I. Moser, *Nature* **436**, 801–806 (2005).
5. K. M. Igarashi, H. T. Ito, E. I. Moser, M.-B. Moser, *FEBS Lett.* **588**, 2470–2476 (2014).
6. M. S. Cembrowski *et al.*, *Cell* **173**, 1280–1292.e18 (2018).
7. P. A. Naber, F. H. Lopes da Silva, M. P. Witter, *Hippocampus* **11**, 99–104 (2001).
8. N. Tamamaki, Y. Nojyo, *J. Comp. Neurol.* **353**, 379–390 (1995).
9. D. S. Berns, L. A. DeNardo, D. T. Pederick, L. Luo, *Nature* **554**, 328–333 (2018).
10. J.-P. Silva *et al.*, *Proc. Natl. Acad. Sci. U.S.A.* **108**, 12113–12118 (2011).
11. M. L. O'Sullivan *et al.*, *Neuron* **73**, 903–910 (2012).
12. A. A. Boucard, S. Maxeiner, T. C. Südhof, *J. Biol. Chem.* **289**, 387–402 (2014).
13. J. Li *et al.*, *Cell* **173**, 735–748.e15 (2018).
14. R. Sando, X. Jiang, T. C. Südhof, *Science* **363**, eaav7969 (2019).
15. D. del Toro *et al.*, *Cell* **180**, 323–339.e19 (2020).
16. G. R. Anderson *et al.*, *J. Cell Biol.* **216**, 3831–3846 (2017).
17. V. A. Jackson *et al.*, *Structure* **23**, 774–781 (2015).
18. Y. C. Lu *et al.*, *Structure* **23**, 1678–1691 (2015).
19. T. C. Südhof, *Neuron* **100**, 276–293 (2018).
20. R. Sando, T. C. Südhof, *eLife* **10**, e65717 (2021).
21. A. L. Kolodkin, M. Tessier-Lavigne, *Cold Spring Harb. Perspect. Biol.* **3**, a001727 (2011).
22. J. R. Sanes, S. L. Zipursky, *Cell* **181**, 536–556 (2020).
23. Z. Wu *et al.*, *Neuron* **70**, 281–298 (2011).
24. M.-A. Lambot, F. Depasse, J.-C. Noel, P. Vanderhaeghen, *J. Neurosci.* **25**, 7232–7237 (2005).
25. J. Cang, D. A. Feldheim, *Annu. Rev. Neurosci.* **36**, 51–77 (2013).
26. J. Egea, R. Klein, *Trends Cell Biol.* **17**, 230–238 (2007).
27. D. T. Pederick *et al.*, Reciprocal-repulsions-instruct-the-precise-assembly-of-parallel-hippocampal-networks, version 1, Zenodo (2021), https://doi.org/10.5281/zenodo.4716610.

ACKNOWLEDGMENTS

We thank T. Südhof for the *Lphn2*^{mVenus} and *Lphn2*^{fl} mice; the Neuroscience Gene Vector and Virus Core at Stanford University for producing viruses; D. Berns for advice, inspiration, and artwork; J. Ferguson for artwork; J. Kebschull for MATLAB code; H. Meng for virus preparation; members of the Luo laboratory for advice and support; and D. Berns, J. Kebschull, A. Khalaj, H. Li, J. Li, T. Li, C. McLaughlin, K. Shen, and A. Shuster for critiques of the manuscript. **Funding:** D.T.P. was supported by an American Australian Association Education Fund Scholarship. J.H.L. is supported by a National Institutes of Health grant (K01-MH114022). L.L. is an investigator of Howard Hughes Medical Institute. This work was supported by National Institutes of Health grant (R01-NS050580 to L.L.). **Author contributions:** D.T.P. performed all of the experiments and analyzed the data, except for single-cell sequencing sample collection and data processing, which were performed by J.H.L., with support from S.R.Q. E.C.G. and C.X. assisted in tissue processing. M.J.W. generated MATLAB code and analyzed data. Y.L. and Z.H. produced custom lentivirus. L.L. supervised the study. D.T.P., J.H.L., and L.L. wrote the paper. **Competing interests:** The authors declare no competing interests. **Data and materials availability:** The sequencing datasets generated in this study are available in the NCBI Gene Expression Omnibus under accession number GSE162552. Custom analysis codes are available at https://github.com/dpederick/Reciprocal-repulsions-instruct-the-precise-assembly-of-parallel-hippocampal-networks or Zenodo (*27*). All other data are available in the main paper and the supplementary materials. All materials are available through requests to the corresponding author.

SUPPLEMENTARY MATERIALS

science.sciencemag.org/content/372/6546/1068/suppl/DC1
Materials and Methods
Figs. S1 to S11
Table S1
References (*28*–*41*)
MDAR Reproducibility Checklist

View/request a protocol for this paper from *Bio-protocol*.

15 December 2020; accepted 27 April 2021
10.1126/science.abg1774

Reciprocal repulsions instruct the precise assembly of parallel hippocampal networks

Daniel T. Pederick, Jan H. Lui, Ellen C. Gingrich, Chuanyun Xu, Mark J. Wagner, Yuanyuan Liu, Zhigang He, Stephen R. Quake and Liqun Luo

Science **372** (6546), 1068-1073.
DOI: 10.1126/science.abg1774

Keeping brain development untangled

Brain circuits established during development can be overlapping or parallel as needed. Pederick *et al.* analyzed how parallel circuits in the mouse medial and lateral hippocampus develop without getting tangled up. Regulated expression of the cell surface molecules teneurin-3 (Ten3) and latrophilin-2 (Lphn2) keeps confusion at bay. Together, these factors act as a membrane-bound ligand-receptor pair with repulsive outcomes, and they are able to destabilize a nascent but incorrect axon-target interaction. Individually, they each mediate homophilic attraction as axons search for their favored targets.

Science, abg1774, this issue p. 1068